

Synchrotron x-ray modification of nanoparticle superlattice formation

Chenguang Lu, Austin J. Akey, and Irving P. Herman

Citation: *Appl. Phys. Lett.* **101**, 133109 (2012); doi: 10.1063/1.4752239

View online: <http://dx.doi.org/10.1063/1.4752239>

View Table of Contents: <http://apl.aip.org/resource/1/APPLAB/v101/i13>

Published by the [American Institute of Physics](#).

Related Articles

X-ray diffraction analysis and Monte Carlo simulations of CoFeB-MgO based magnetic tunnel junctions
J. Appl. Phys. **113**, 023915 (2013)

X-ray small-angle scattering from sputtered CeO₂/C bilayers
J. Appl. Phys. **113**, 024301 (2013)

Reactive sputter magnetron reactor for preparation of thin films and simultaneous in situ structural study by X-ray diffraction
Rev. Sci. Instrum. **84**, 015102 (2013)

Probing ballistic microdrop coalescence by stroboscopic small-angle X-ray scattering
Appl. Phys. Lett. **101**, 254101 (2012)

Exploration of precessional spin dynamics in magnetic multilayers
J. Appl. Phys. **112**, 103914 (2012)

Additional information on *Appl. Phys. Lett.*

Journal Homepage: <http://apl.aip.org/>

Journal Information: http://apl.aip.org/about/about_the_journal

Top downloads: http://apl.aip.org/features/most_downloaded

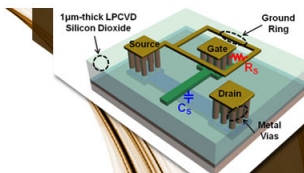
Information for Authors: <http://apl.aip.org/authors>

ADVERTISEMENT



**EXPLORE WHAT'S
NEW IN APL**

SUBMIT YOUR PAPER NOW!



SURFACES AND INTERFACES

Focusing on physical, chemical, biological, structural, optical, magnetic and electrical properties of surfaces and interfaces, and more...



ENERGY CONVERSION AND STORAGE

Focusing on all aspects of static and dynamic energy conversion, energy storage, photovoltaics, solar fuels, batteries, capacitors, thermoelectrics, and more...

Synchrotron x-ray modification of nanoparticle superlattice formation

Chenguang Lu, Austin J. Akey, and Irving P. Herman^{a)}

Department of Applied Physics and Applied Mathematics, Columbia University, New York, New York 10027, USA

(Received 26 July 2012; accepted 29 August 2012; published online 27 September 2012)

The synchrotron x-ray radiation used to perform small angle x-ray scattering (SAXS) during the formation of three-dimensional nanoparticle superlattices by drop casting nanoparticle solutions affects the structure and the local crystalline order of the resulting films. The domain size decreases due to the real-time SAXS analysis during drying and more macroscopic changes are visible to the eye. © 2012 American Institute of Physics. [<http://dx.doi.org/10.1063/1.4752239>]

Synchrotron x-ray radiation can be used for materials processing and analysis when large x-ray fluxes and high spatial resolution are needed. As a processing tool, such irradiation has been used in studies of resist exposure¹ and resist direct patterning² for x-ray lithography. As a diagnostic tool, this irradiation should lead to no physical or chemical changes to the probed region, though sometimes it does. For example, synchrotron microbeams of x-rays (11.2 keV) used for diffraction damage the thin Si layers of silicon-on-insulator (SOI) structures, possibly due to the formation of nonradiative defects at the Si/SiO₂ interface and probably not due to heating.³ Synchrotron irradiation (8.6 keV) of submicron Cu interconnect structures encapsulated by organosilicate glass causes a densification and an increase in elastic modulus of the low-k dielectric film and the generation of stress and strain, as monitored by diffraction of this probing x-ray beam.⁴ While it is clear that high x-ray fluxes and fluences can lead to damage when probing a material *ex situ* after processing, it is less clear exactly how such real-time x-ray exposure affects materials processing itself, such as the assembly of nanoparticles (NPs) or nanocrystals. We have demonstrated that the mm-dimension synchrotron x-ray beam used for real-time, small-angle x-ray scattering (SAXS) analysis of the formation of thick large-area three-dimensional (3D) superlattices of NPs [or supercrystals (SCs)] can have the unintended effect of modifying the structure of the SC formed, decreasing the effective domain size.

Synchrotron x-rays have been used in several SAXS studies of NP superlattice (SL) formation, both *ex situ* and *in situ*. For example, Smith *et al.* performed grazing incidence SAXS on large area binary particle superlattices *ex situ*⁵ and Jiang *et al.* performed grazing incidence SAXS on large-area two-dimensional superlattices of Au nanoparticles *in situ*.⁶ We have previously reported on the *ex situ* SAXS analysis of supercrystals formed by drying of solutions of nanocrystals that had been entrained into capillary channels.⁷

Films were formed by drop casting a solution of 13.8 nm diameter magnetite NPs in 72% toluene, 22% decane, and 6% dodecane solvent on a substrate (Si or Kapton); the samples were dried under vacuum with steady-state pressure ~ 150 Torr to form ~ 1 μm thick films. NPs were prepared as described in Ref. 7. SAXS was performed periodically

during drying using the NSLS SAXS beamline X9 at the Brookhaven National Laboratory (14.5 keV x-rays, average photon flux of $\sim 4.5 \times 10^{10}/\text{s}$, 3×10^{-10} s long pulses, at $\sim 4 \times 10^7$ Hz) with beams that were $1.5 \text{ mm} \times 10 \mu\text{m}$ at the sample (and $1.5 \text{ mm} \times \sim 5 \text{ mm}$ and $1.5 \text{ mm} \times \sim 3.5 \text{ mm}$ projected on the inclined stationary and repositioned substrates described below). The evolution of the SCs was monitored, and will be reported in detail elsewhere. Only the effect of x-ray exposure will be reported here.

In initial studies, x-rays impinged at a 0.35° angle on one spot on a stationary Si substrate, with 20 s x-ray exposures separated by 5 s, for a total exposure of 1000 s. The reflected and transmitted beams were both detected by a charge-coupled device (CCD) array. SAXS traces showed that an ordered array of NPs formed during drying.

A streak is visible to the naked eye on these samples; this appears as a light streak in the optical micrograph in Fig. 1, at the site of the x-ray beam irradiation and with the same width as the incident x-ray beam. This modification of the NP film raises concerns about the utility and interpretation of the SAXS data. Scanning electron microscopy (SEM) and atomic force microscopy (AFM) do not show differences in the supercrystal periodicity, the number of defects, or the thickness of the film in irradiated regions. Optical microscopy shows that the surface is not visibly thicker or thinner within

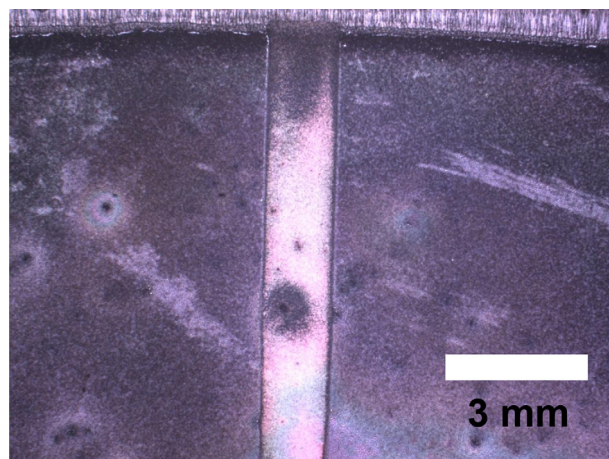


FIG. 1. Optical micrograph of a supercrystal film of magnetite NPs formed on a stationary Si substrate (with the wafer edge on top) by drying in the vacuum chamber during real-time SAXS measurements. A light, 1.5 mm wide streak is visible on the film where the x-ray beam is incident.

^{a)} Author to whom correspondence should be addressed. Electronic mail: iph1@columbia.edu.

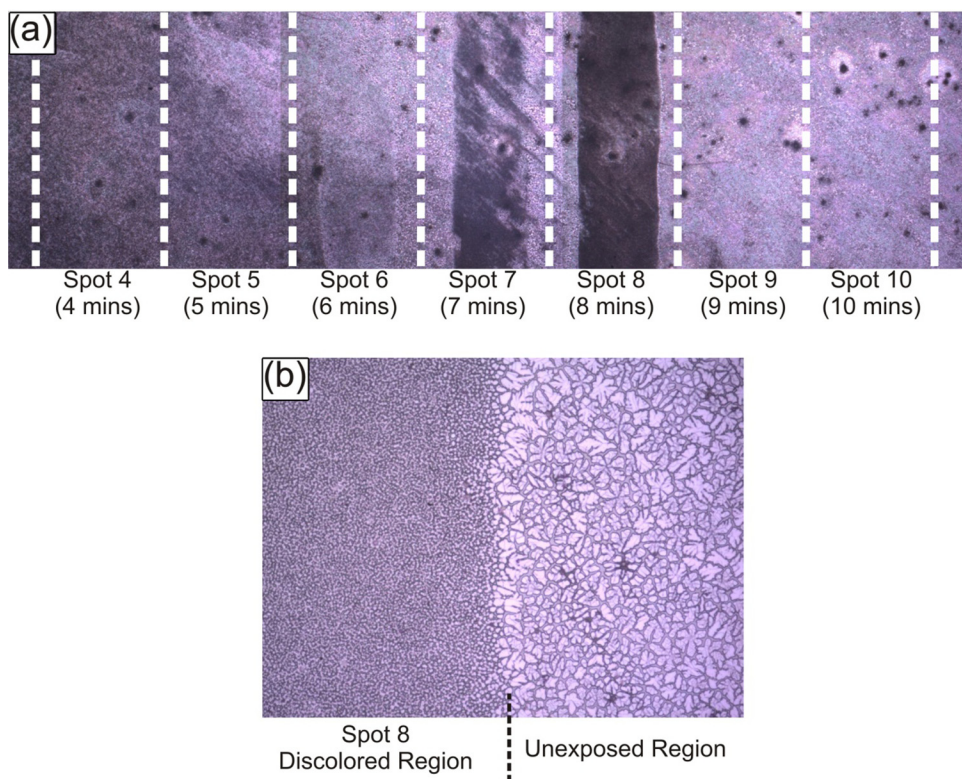


FIG. 2. Optical micrograph of a Kapton film substrate with a supercrystal film formed during real-time SAXS measurements, with 20-s long exposures followed by substrate repositioning. (a) Indicated are the locations of seven of the 12 measured spots on this sample; Spots 6, 7, and 8, which correspond to the times where crystallization was observed in SAXS (see Fig. 4), are darkened. The space between dashed lines corresponds to 2 mm. The film formed on a Si substrate looks similar. (b) High-magnification, 1-mm wide micrograph of Kapton film substrate showing the discolored region of Spot 8 (on the left) and unexposed region (on the right).

the discolored area. Similar exposures of already-dried SC films and of substrate regions without any film show no such discoloration. In addition, streaks are seen in the real-time SAXS image in the q_z direction, which suggests lack of local order in the z direction.

Experiments were restructured to better characterize the interaction causing this discoloration and to prevent, or at least minimize, any effect it might have on the SAXS analysis. A series of ~ 12 measurements were performed with 20 s exposures, separated by 40 s, with each measurement made on a fresh section of the drying film that had not been previously irradiated by the x-ray beam. Even if the measurement were to affect the supercrystal locally, each measurement would be made on a pristine area. This repositioning was done with a Si substrate and, to decrease signal losses for transmission SAXS, also with a Kapton substrate. A strip of the same Kapton film (~ 0.1 mm thick) used for the x-ray windows of the vacuum chamber, which is an x-ray-transparent polymer that is highly resistant to the solvents employed here, was used. This film was slightly creased to prevent small distortions in its shape from making the NP solution pool unevenly. It was then suspended between two posts inside the vacuum chamber, and the NP solution was depos-

ited and the chamber sealed and pumping was begun. The sample was inclined to an angle of 5° from horizontal, and the x-ray beam aligned to pass through the center of the substrate and the NP solution drop to ensure that the CCD array would see only the SAXS transmitted signal. (The reflected and transmitted beams overlapped on the CCD array with the previous geometry. Transmission SAXS data are shown for the experiments presented below.) With the stage and Kapton substrate fixed during exposure, the visible streaks and the streaks in the SAXS image were the same as with the stationary Si substrate.

With the substrate repositioned between exposures, three or four discolored spots were typically visible, out of the ~ 12 total spots studied during the drying. Figure 2(a) is an optical micrograph showing the locations of 7 of the 12 spots measured on one sample for a Kapton substrate. Spots 6, 7, and 8 correspond to the times when crystallization is first evident (as seen in Fig. 4 below) and only at these times is there a discoloration on the film similar to that seen in Fig. 1. Similar discolorations were seen with Si substrates. These discolored regions (which are darkened regions for Kapton) look the same as the undamaged regions when examined with AFM, but look different with SEM Fig. 3.

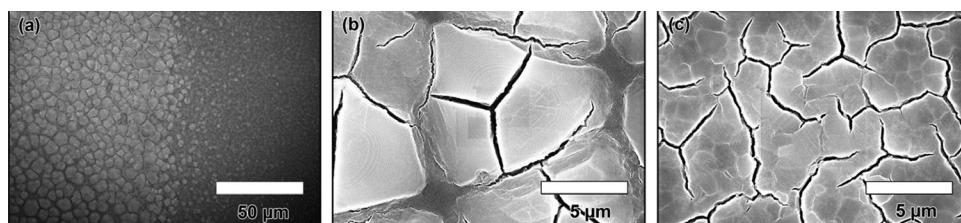


FIG. 3. SEM micrograph of a Si substrate with a supercrystal film formed during real-time SAXS measurements, with 20-s long exposures followed by substrate repositioning. Image (a) compares regions without x-ray irradiation (left in (a), expanded in (b)) and with x-ray irradiation (right in (a), expanded in (c)), which has smaller SC domains, with $\sim 1 \mu\text{m}$ lateral dimension.

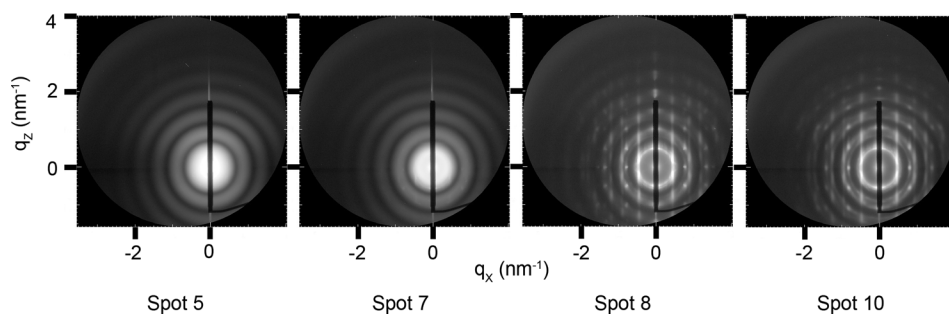


FIG. 4. SAXS in transmission for several of the spots shown in Fig. 2, with Spot 5 before, Spots 7 and 8 during, and Spot 10 after drying of the NP film. fcc ordering is seen in Spots 8 and 10.

(Because of charging, only the Si substrates could be studied by SEM.) Typical SAXS data for spots before, during, and after discoloration are shown in Fig. 4. As with the stationary Si substrates, for these repositioned substrates similar studies performed on a dried film and on regions without any film show no discoloration. This discoloration seen during the formation of 13.8 nm NP SLs was also seen during the drying of mixtures of 5.9 nm and 12.4 nm diameter magnetite NPs that formed binary particle superlattices.

The onset of modification in the spots in Fig. 2 corresponds to the onset of vertical streaks in the SAXS images; these vertical streaks are believed to correspond to the first sign of ordering of the NPs. The appearance of visible streaks in these images ceases after narrow rings have formed in the SAXS images, indicative of long-range 3D ordering. Spots corresponding to SAXS data that indicate the amorphous and post-drying crystalline phases are not discolored. This implies that the sample is most sensitive to the beam during supercrystal formation, and that the discoloration stems from some change in the supercrystal itself.

Figure 2(b) shows a higher magnification optical micrograph of Spot 8 and the unirradiated region to the right of it. The film in the exposed, discolored region possesses a much finer, rougher microstructure than that in the unexposed region. This is similar to what is seen for irradiation during the entire drying period on stationary Si substrates. The average island size in the irradiated region in Fig. 2(b) is $\sim 8 \mu\text{m}$, while that in the unirradiated region on the right is $\sim 30 \mu\text{m}$. The higher resolution, SEM images in Figs. 3(b) and 3(c) show the structure in more detail for Si substrates: a lateral SC domain size in the irradiated region (Fig. 3(c)) of $\sim 1 \mu\text{m}$ within larger $\sim 3 \mu\text{m}$ dimension regions defined by cracks, while in the unirradiated region (Fig. 3(b)) the SC domain size is $\sim 10 \mu\text{m}$, but it cracks into smaller $\sim 5 \mu\text{m}$ islands. SEM analysis at higher magnification shows that the surface of these domains are periodic, suggesting that each domain is a supercrystal.

Fracture is observed in these thick films both with and without x-ray irradiation because of the strain that develops due to solvent evaporation. Irradiation decreases the size of the single supercrystalline domains, likely due to an increased density of nucleation sites. X-ray irradiation could create charges by ionization in either NP cores or ligands; alternatively, irradiation could decompose the NP capping ligands which could create additional sites for nucleation of SC islands or lead to faster aggregation of the NPs (due to reduced screening between their surfaces) or to a reduction in their solubility in the solvents. X-ray heating is not thought to be important.

The SAXS data indicate supercrystal ordering (fcc-like structure for these 13.8 nm magnetite NPs) in the nonirradiated and discolored regions. There is always the same in-plane structure in both, but there is additional vertical (q_z) streaking in the discolored regions, which indicates some disorder in the z direction. The lateral domain size is always large enough not to broaden the x-ray features.

This last series of experiments was repeated using a Kapton substrate and much shorter, 3-s long, x-ray exposures between repositioning. No visible streaks on the sample and little streaking in the q_z in the SAXS images are seen. There is still some slight elongation in the q_z directions, which indicates the small degree of disorder in the z direction that is always seen independent of analysis conditions. No detectable changes are seen with optical microscopy with 3-s long exposures.

In conclusion, we have seen that synchrotron x-ray irradiation during drop casting of NP solutions can change the structure of the nanoparticle superlattice films that form. The domain size decreases and the supercrystal becomes somewhat disordered in the z direction. Shorter duration exposure mitigates these effects, as would the use of even lower x-ray fluxes; however, challenges may arise when using the more tightly focused synchrotron beams that could improve spatial resolution. Details regarding the supercrystal formation and structure will be presented elsewhere.

The authors thank I. Cev Noyan for valuable discussions. This work was supported primarily by the MRSEC program of the National Science Foundation (DMR-0213574), the NSEC program of the NSF (CHE-0641523), the EFRC program of DoE (DE-SC0001085), and by the New York State Office of Science, Technology, and Academic Research (NYSTAR). Use of the Center for Functional Nanomaterials at Brookhaven National Laboratory, was supported by the U.S. Department of Energy, Office of Science, Office of Basic Energy Sciences, under Contract No. DE-AC02-98CH10886.

¹J. P. Silverman, *J. Vac. Sci. Technol. B* **16**, 3137 (1998).

²T. C. Chang, T. M. Tsai, P. T. Liu, Y. S. Mor, C. W. Chen, Y. J. Mei, J. T. Sheu, and T. Y. Tseng, *Thin Solid Films* **420–421**, 403 (2002).

³S. M. Polvino, C. E. Murray, Ö. Kalenci, I. C. Noyan, B. Lai, and Z. Cai, *Appl. Phys. Lett.* **92**, 224105 (2008).

⁴C. E. Murray, P. R. Besser, E. T. Ryan, and J. L. Jordan-Sweet, *Appl. Phys. Lett.* **98**, 141916 (2011).

⁵D. K. Smith, B. Goodfellow, D.-M. Smilgies, and B. A. Korgel, *J. Am. Chem. Soc.* **131**, 3281 (2009).

⁶Z. Jiang, X.-M. Lin, M. Sprung, S. Narayanan, and J. Wang, *Nano Lett.* **10**, 799 (2010).

⁷A. Akey, C. Lu, L. Yang, and I. P. Herman, *Nano Lett.* **10**, 1517 (2010).